

Practical Works (TP4b) : Studying the Large Scale Structure with Voids

Pierre Boccard

Andrei Variu, Cheng Zhao, Amelie Tamone, Daniel Forero

9 November 2022

ABSTRACT

In this report, we detail our project that focused on testing whether numerical models could be used to extract cosmological information from the clustering of voids. We present an analysis of the RSD effect using a multipole decomposition of the void-galaxy cross-correlation using a Big MultiDark simulation. We compute numerically the void cross-correlation with galaxies in redshift space and compare it to a theoretical Redshift Space Distortion (RSD) model that we compute by finding its cosmological parameters. The parameters that we compute in this project are the average mass density contrast, the void cross-correlation with galaxies in real space and the velocity dispersion profile of galaxies. We also compute the void density contrast and the average (stacked) galaxy velocity profile projected on the void-galaxy separation vector.

1 INTRODUCTION

Astronomical observations at low redshifts, namely sky surveys and mappings in a broad range of wavelengths, help scientists yield information on the content and character of the universe’s structure. It reveals that our present Universe has large scale structures of matter organized into galaxies, which in turn form galaxy groups, galaxy clusters, superclusters and filaments, which span over hundreds of Megaparsecs. These regions of matter are separated by cosmic voids, which are large regions of space with low matter densities, i.e. large under-densities in the galaxy distribution. Thus, they trace stationary points of the gravitational potential where velocities are dominated by coherent bulk flows (Nadathur et al. (2017))

Because they are regions of low density, the expansion of the Universe should not have affected them a lot and thus they could be used as cosmological tools for multiple purposes : to trace cosmic structure formation (Betancort-Rijo et al. (2009)), to constrain cosmological parameters (Sutter et al. (2014)) and to probe the distribution of dark matter and its nature.

Finally, the study of cosmic voids helps present evidence of baryon acoustic oscillations (BAO) signal, which provides additional information than that of galaxies, and is used as a standard ruler for measuring the distance of the Universe (Zhao et al. (2016))

All these key information allow precise tests of the standard cosmological Λ CDM model, which is the model that we use in this project for our numerical simulations.

In our simulations, and as observed in the Universe, galaxies have peculiar velocities which cause the spatial distribution of galaxies to appear squashed and distorted when their positions are plotted as a function of their redshift, this effect is known as Redshift Space Distortion (RSD) effect. In other terms, the growth of the Universe causes these peculiar velocities that affect the measured redshifts of the galaxies which then manifests in additional anisotropies in the galaxy clustering along the line-of-sight. One striking consequence of this effect is the phenomenon of Fingers of God where the galaxies in a cluster seem to be organised in an elongated filament pointing toward the observer in redshift space. This RSD effect can be measured (Peacock et al. (2001)) and used to determine the growth rate of structure, which can provide strong tests of General Relativity (GR)

The theory of RSD in the galaxy clustering is however complicated by significant non-linear contributions which are important even at quite large pair separation scales, requiring sophisticated modelling (Matsubara (2008) Scoccimarro (2004)). This project presents an analysis of the RSD effect using a multipole decomposition of the void-galaxy cross-correlation in different spaces. Previous studies (Cai et al. (2016), Nadathur et al. (2019b)) have shown that the multipole decomposition can accurately describe the cross-correlation in redshift space on all scales. The RSD model of multipoles that we use is based on linear perturbation theory dynamics and a convolution due to dispersion in galaxy velocities around the coherent mean outflow (Nadathur & Percival (2019)). The full description of the model and other complications can be found in (Nadathur et al. (2019a)). This model has proven to describe accurately the cross-correlation in redshift space on all scales.

The aim of this project is to determine if our numerical simulations are in agreement with the linear-theory model with velocity dispersion. To do that we will first compute numerically the void-galaxy cross-correlation function in redshift space and in a second time determine the cosmological parameters of our RSD model : $\Delta(r)$ the average mass density contrast, $\xi_r(r)$ the cross-correlation with galaxies in real space and $\sigma^{gal}(r)$ the velocity dispersion profile of galaxies, that we will describe in detail later, to see if the model follows the previous computations

The rest of this paper is organized as follows. We will present the data that we use, that is to say our numerical simulation, as well as the different programs and methods that we use. Then we will describe in some detail the theoretical RSD model and how to obtain its cosmological parameters. Finally we will present our results and discuss them.

2 DATA AND METHODS

2.1 *N*-body Mocks

The first type of data provided for our project is a mock galaxy catalogue from an *N*-body simulation. The simulation used is the Big MultiDark simulation, which consists of 3840^3 dark matter particles in a box of size of 2500Mpc/h. The simulation was computed with

cosmological parameters $h = 0.6777$, $\Omega_m = 0.307$, $\Omega_\lambda = 0.693$, $\Omega_b = 0.0482$ and $\sigma_8 = 0.8228$ and we take a snapshot of the simulation at redshift $z = 0.5053$. This galaxy catalogue is referred in the rest of this paper as the real space galaxy catalogue. As a matter of fact, the N -body simulation originally provides a density field of dark matter particles. Then this density field was used to obtain the galaxy catalogue.

In this project we will make use of the galaxy catalogue to compute numerically the void-galaxy cross-correlation function in redshift and real space and also $\sigma_{\text{vll}}^{\text{gal}}(r)$ while the original density field of dark matter particles will allow us to compute $\Delta(r)$.

2.2 Catalogue construction

In this part, and for the rest of the project, we will take our model to be flat Λ CDM with cosmological parameters : $\Omega_\Lambda = 0.692885$, $\Omega_M = 0.307115$, $H_0 = 67.77$ and $z = 0.505300$ respectively the mass density of dark energy, the mass density of dark and baryonic matter, the Hubble parameter and the redshift.

2.2.1 Real to redshift space

The first catalogue constructed is the catalogue of galaxies in redshift space, constructed from the catalogue in real space.

In order to do that, we use the following equation which transforms the coordinates in real space X_{real} into coordinates in redshift space X_{redshift} :

$$X_{\text{redshift}} = X_{\text{real}} + (1+z) \cdot \frac{v_{\text{pec}}}{H(z)} \quad (1)$$

with v_{pec} being the velocity of the galaxy in real space. In our case, the galaxies are considering to move along the line the line of sight only in the z direction which means that the only coordinate transformation as described in Eq. (1) is on the z coordinate.

2.2.2 Reconstructed space

Another step in the catalogue construction is the computation of the galaxy catalogue in reconstructed space. In (Nadathur et al. (2019a)), the cross correlation is computed with voids in reconstructed space and galaxies in redshift space. This is done because the theoretical model of the void-galaxy correlation depend on the assumption that the centers of voids are stationary which is not satisfied if the voids are directly identified in the redshift-space galaxy distribution. Thus, as explained in detail in (Nadathur et al. (2019a)), the goal is to reconstruct the approximate real-space galaxy positions by removing the effects of large-scale velocity flows before performing the void-finding explained in 2.2.3.

However in this report we will not make use of the reconstructed space catalogue but it would be interesting in future projects to use it.

2.2.3 Void finding

Finally, having the galaxy catalogues in real, redshift and reconstructed space, we can now perform the void-finding of these catalogues. Void-finding is performed using the Delaunay triangulation Void findEr (DIVE) code provided based on the Delaunay Triangulation technique (B. Delaunay (B. Delaunay)). Further details about the DIVE code can be found in (Zhao et al. (2016)). Using the Delaunay Triangulation technique which generates meshes to discretise

a spatial domain, the DIVE code allows us to compute the empty spheres constrained by a discrete set of tracers. In our project, these spheres are regions of our spaces called DT voids and they are empty of tracers, here galaxies. Thus, DIVE allows us to obtain three voids catalogue in real, redshift and reconstructed space.

2.3 Fast Correlation Function Calculator

The second computational code provided is the Fast Correlation Function Calculator (FCFC), that we will use on our different catalogues. It will allow us to determine the real space galaxy cross-correlation $\xi_r(r)$ needed to construct our model as well as the redshift space galaxy cross-correlation $\xi_s(r)$ that we compare to the model.

3 THEORY

In this project we make use of the theoretical model for RSD in the void-galaxy cross-correlation developed in (Nadathur et al. (2019a)), which we will describe briefly. As mentioned previously, the calculation of this model $\xi^{s,th}(s, \mu)$ requires specification of three functions in real space that are not known a priori. We have seen how to obtain the first one $\xi_r(r)$ and will now see how to obtain the two remaining functions, namely $\Delta(r)$ and $\sigma_{\text{vll}}^{\text{gal}}(r)$.

3.1 The void-galaxy cross-correlation

The real space separation vector for the void-galaxy pair is denoted by \mathbf{r} while the one for redshift space is denoted by \mathbf{s} . Considering we are distant observers, we make the assumption the void centre position is invariant under the RSD mapping and that both vectors are related by the following relation :

$$\mathbf{s} = \mathbf{r} + \frac{\mathbf{v}_g \cdot \mathbf{r}}{aH} \quad (2)$$

thus considering that the transformation solely depends on the galaxy velocity v_g while the void velocity is considered to be zero. Here $H = H(z)$, the Hubble parameter at redshift z . Similarly, the cross-correlation with galaxy positions in real space is noted $\xi^r(r)$ and $\xi^s(r)$ in redshift space. Under the further assumptions that galaxy velocities around the void centre are determined by linear dynamics, depend only on the void itself rather than other structures in the environment, and show spherical symmetry around the void centre, we may write

$$\mathbf{v}_g = -\frac{1}{3} f a H \Delta(r) r \hat{\mathbf{r}} \quad (3)$$

with $\Delta(r)$ the average mass density contrast within radius r of the void center.

3.1.1 Density contrast

We now focus on how to evaluate this parameter $\Delta(r)$, the average mass density contrast. It is defined by the equation :

$$\Delta(r) \equiv \frac{3}{r^3} \int_0^r \delta(y) y^2 dy \quad (4)$$

where $\delta(r)$ is the (isotropic) average mass density profile of the void. To compute the integral we will approximate it using the trapezoidal rule which follows the method :

$$\int_0^r \delta(y)y^2 dy = \sum_{i=1}^{N-1} \frac{(\delta_{i+1} \cdot x_{i+1}^2 + \delta_i \cdot x_i^2)}{2} \cdot (x_{i+1} - x_i) \quad (5)$$

We thus need to determine $\delta(r)$, which we will do using the FCFC code to compute the density field-void cross-correlation. As we are looking for the mass density around voids as a function of the distance to the center, we compute the cross-correlation of the voids' center with the dark matter particles, as these particles give us the mass distribution.

We now have another cosmological parameter of our model that we were looking for. The following step is to obtain the final parameter, the dispersion of of galaxies velocities in the line-of-sight profile $\sigma_{v_{\parallel}}^{gal}(r)$.

3.2 Dispersion velocity profile

First of all, $\sigma_{v_{\parallel}}^{gal}(r)$ is given by :

$$\sigma_{v_{\parallel}}^{gal}(r) = \left[\frac{1}{N_{vg}} \sum_{i,j} \left(\mathbf{v}_j \cdot \mathbf{X}_j - \bar{v}_{\parallel}(r)^2 \right) \right]^{1/2} \quad (6)$$

In practice, to compute $\sigma_{v_{\parallel}}^{gal}(r)$ we use the FCFC code. We need to compute 3 terms that we combine by using weighted pair-counts :

- N_{vg} the pair-count of all void-galaxy pairs with $|r|$ within $(r \pm dr)$
- $\sum_j v_j \cdot \mathbf{X}_j$ which is the galaxy velocity profile around the void centers projected on the line-of-sight X_j . The line of sight direction is the same for all galaxies in the plane-parallel approximation and taken to be along the z-axis of the simulation box.
- $\bar{v}_{\parallel}(r)^2$ is the mean line of sight velocity component at r

3.3 Theoretical model

We now have the three functions allowing us to compute our base model.

Since void-galaxy pairs are a conserved quantity, we can use this information and combine it with equation (2), (3) and (4), to obtain the relation :

$$1 + \xi^s(s) = (1 + \xi^r(r)) \left[1 - \frac{f\Delta(r)}{3} - f\mu^2(\delta(r) - \Delta(r)) \right]^{-1} \quad (7)$$

where $\mu = \frac{\mathbf{X} \cdot \mathbf{r}}{|\mathbf{X}|r}$ is the cosine of the angle between the void-galaxy separation vector and the line-of-sight direction. After doing a series expansion and extending it to take into account for dispersion in line-of-sight galaxy velocities v_{\parallel} , we obtain the final and full model :

$$1 + \xi^{s,th}(s, \mu) = \int_{-\infty}^{\infty} \frac{\left(1 + \xi^{s,base}(s_{\perp}, s_{\parallel} - v_{\parallel}/aH) \right)}{\sqrt{2\pi}\sigma_{v_{\parallel}}(r)} \exp\left(\frac{-v_{\parallel}^2}{2\sigma_{v_{\parallel}}^2(r)} \right) dv_{\parallel} \quad (8)$$

with $s_{\parallel} = s\mu$ and $s_{\perp} = s\sqrt{1 - \mu^2}$ being the the components of the

vector s parallel and perpendicular to the line of sight respectively, r is the real-space void-galaxy separation distance

$$r = \sqrt{s_{\perp}^2 + \left(s_{\parallel} + \frac{s_{\parallel} - v_r(r)\mu}{aH} \right)^2} \quad (9)$$

4 RESULTS

4.1 Cross-correlations

For the rest of the project, to denote the choice of space chosen for galaxies and voids, we will always mention the space for galaxy first. Thus, "redshift-real space" means that the galaxies are in redshift space and voids in real space.

Furthermore, our cross-correlation computations will be done on multiple void's radius intervals such as (8, 50), (12, 50), (16, 50) and (20, 50) Mpc/h. However, as shown by (Zhao et al. (2016)) the interval of interest is (16,50) Mpc/h. They explain that the value of 16 Mpc/h is a cut to be sure that the voids are tracking under-densities because smaller voids track over-densities, that is to say where there lot of galaxies.

4.1.1 Real-real space

The first cross-correlation computation is naturally done on galaxies and voids in real space and presented on Fig. 1 with the monopole on the left panel and quadrupole on right panel. This will provide us with the first parameter of our model $\xi_r(r)$. The monopole ξ_0^s is multiplied by s^2 in order to see more precisely its shape for large s . Indeed, ξ_0^s converges to 0 for $s > 40$ very rapidly and is barely visible and this behaviour is the same regardless of the radius interval taken for the voids. This same method is also done for the following cross-correlation computations.

As seen on the left panel of Fig. 1, the quadrupole moment is very small, of order 10^{-3} , and can be neglected. The behaviour is expected because, in real space the Universe is isotropic and the quadrupole moment should thus be zero. Indeed this comes from the construction of our multipole moments : $\xi_l(s) \equiv \frac{2l+1}{2} \int_{-1}^1 L_l(\mu)\xi(s, \mu)d\mu$, where $L_l(\mu)$ is the Legendre polynomial of order l . Thus the assumption of statistical isotropy means that for the real-space correlation $\xi^r(r) = \xi_0^r(r)$.

4.1.2 Redshift-real space

The second galaxy-voids cross-correlation computed is done in redshift-real space and presented on Fig. 2 with again the monopole on the left panel and quadrupole on right panel. This cross-correlation will be later compared to our theoretical model.

This time the left panel on Fig. 2 shows as expected that the quadrupole moment is not negligible. Indeed, as explained previously, the RSD effect causes anisotropies in the galaxy clustering in redshift space which implies a non-zero quadrupole moment. Looking at the plot, we see that there is a hollow in the curve for both monopole and quadrupole at distance $s \approx 18\text{Mpc/h}$. A similar hollow is also observed for the monopole moment of the real space cross-correlation on the left panel of Fig. 1.

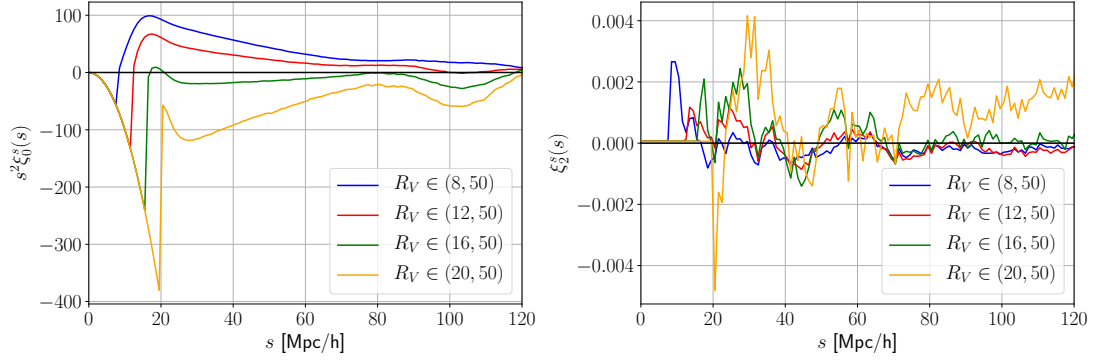


Figure 1. Multipole moments of the real space galaxy-void cross-correlation function from the Big MultiDark simulation. The panels show (left) the monopole moment, $s^2 \xi_0^s$, and (right) the quadrupole moment, ξ_2^s , of the three-dimensional void-galaxy cross-correlation ξ^s , as functions of the radial void-galaxy separation s

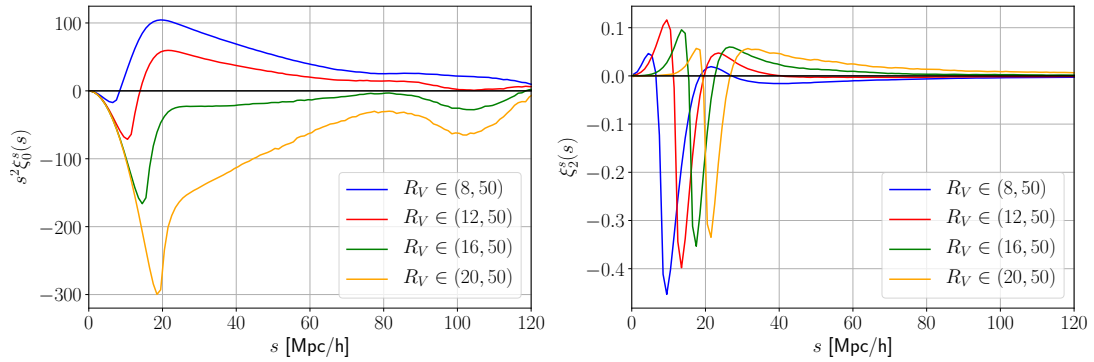


Figure 2. Multipole moments of the redshift-real space galaxy-void cross-correlation function from the Big MultiDark simulation. The panels show (left) the monopole moment, $s^2 \xi_0^s$, and (right) the quadrupole moment, ξ_2^s , of the three-dimensional void-galaxy cross-correlation ξ^s , as functions of the radial void-galaxy separation s

4.2 Density contrast

As explained in 3.1.1, we compute the voids-density cross-correlation in order to obtain the density contrast $\delta(r)$ as a function of the distance to the voids' center and present it on Fig. 3. In a similar approach as (Nadathur & Percival (2019)), we have divided the separation r by the minimal value of void's radius R_V in our interval, thus for the interval (16,50) Mpc/h, we divide by 16. (Nadathur & Percival (2019)) on the other hand divided by the mean radius voids \bar{R}_V . The quantities are similar since 3 of our intervals are narrow while the last one, (16,50), has a mean void's radius of 18 which is not too far from 16. Again, our interval of interest is for voids bigger than 16Mpc/h, which corresponds to the green curve on Fig. 3. As we can see, the green curve does not have a peak for $r/R_V^{min} \approx 1$, whereas the other curves do.

Now that we have δ we can compute the average mass density contrast $\Delta(r)$ using equations (4) and (5) and present it on Fig. 4. Looking at the plot, we see that all curves have a hollow around $r/R_V 8$ and increase to tend to 0 for larger values of r/R_V . We see again that for our radius interval of interest (16, 50) Mpc/h, the mass density contrast $\Delta(r)$ never becomes positive and tend to 0 while staying negative, which is not a behaviour we observe for intervals such as (8, 50) or (12, 50) Mpc/h.

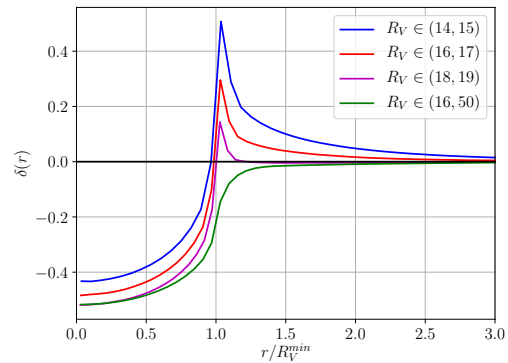


Figure 3. Void density contrast δ as function of r/R_V^{min} the distance from the centre of the void divided by the minimal value of void's radius in the interval

4.3 Velocity profiles and dispersion

Fig. 5 presents the final parameter of our model $\sigma_{v_{||}}^{gal}(r)$ obtained with equation (6). We can see that the curve increases for small r/R_V^{min} then reaches a maximum value around 353km/s and remains constant. We can note that the first values of $\sigma_{v_{||}}^{gal}(r)$, for $r/R_V^{min} < 1$ are not plotted because they are 0. Indeed, for distance s smaller than 16Mpc/h, there are no pairs counted.

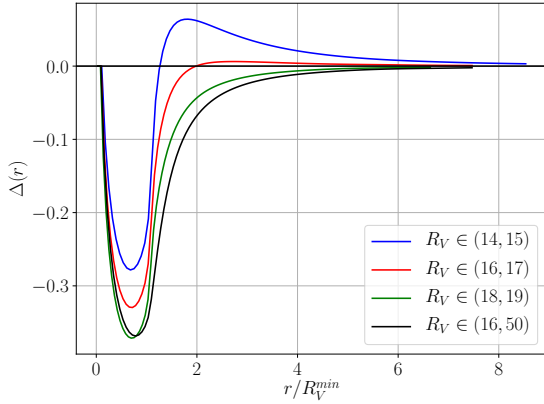


Figure 4. Average mass density contrast within radius r of the void center

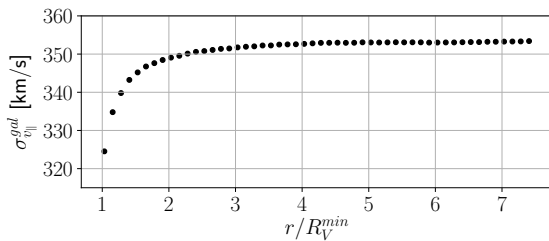


Figure 5. The computed dispersion of galaxy line-of-sight velocities $\sigma_{v_{||}}^{gal}(r)$

Finally, we compare on Fig. 6 the void-matter correlation $\delta(r)$ and the galaxy velocity dispersion profile in the same way (Nadathur et al. (2019a)) did in their study. We add the value 1 to void-matter correlation $\delta(r)$ and normalize the velocity dispersion profile by its asymptotic value at large distance which is, as we can see on Fig. 5, around 352km/s. We observe on the plot that both curves start to overlap for distances $r > 16\text{Mpc}/h$ and reach the same asymptotic value at large distances. The velocity dispersion profile (red curve) is null for $r < 16\text{Mpc}/h$ which explains the vertical behaviour at $r = 16\text{Mpc}/h$.

4.4 Theoretical model

The final part of this project is to present the theoretical RSD model that we can compute now that we have our 3 unknown parameters, and compare it to the redshift space galaxy cross-correlation with voids to see if it matches. The monopole (left) and quadrupole (right) moment of the theoretical model and the computed redshift space cross-correlation are presented on Fig. 7. Note that the redshift space cross-correlation in red is exactly the same function as the one presented on Fig. 2.

Looking at the monopole moment, we can see that the RSD model follows very closely the computed cross-correlation ξ_{gv} . We note that both curves overlap up to $s \approx 120\text{Mpc}/h$ and then separate themselves. This is expected because the computations of our parameters σ , Δ were done for $s < 120\text{Mpc}/h$. The discrepancy in the shape of the curves at $s \approx 25\text{Mpc}/h$ could be explained by a small error in one parameter or an imprecision in the integrating process of the RSD model.

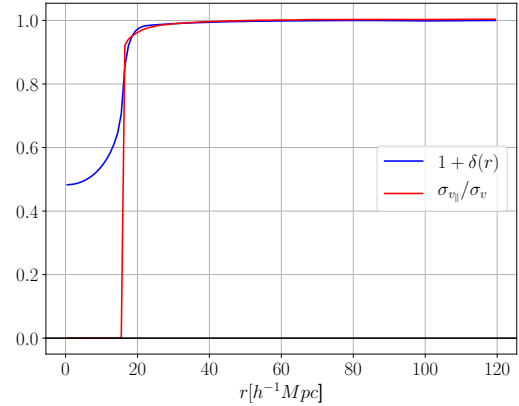


Figure 6. The void-matter correlation $1 + \delta(r)$ (blue) and galaxy velocity dispersion profile (red). Both are measured as angle-averaged functions of the real-space distance from the void centre, r . The dispersion profile is shown normalized by its asymptotic value at large distances

On the other hand, the quadrupole moment does not follow very well the cross-correlation ξ_{gv} . Both curves present a similar hollow at around $20\text{Mpc}/h$ and then separate and the value of the quadrupole moment of our model is slightly smaller than the measured quadrupole. However, we see that their behaviour is not completely different as they both present a peak around roughly $25\text{Mpc}/h$ and then decrease slowly as s increases.

5 DISCUSSION

If we would to continue further in our project, some improvements could be made regarding the methods and the computations. First of all, as explained in 2.2.2, it would be necessary to use the galaxy catalogue in reconstructed space, which would allow us to be independent from the assumption made that the centers of voids are stationary. In addition, it could have been useful to find a way to make sure the construction of our galaxy catalogue in redshift space is correct.

Regarding our theoretical model and the comparison with the measured cross-correlation, the results for the monopole moment are very satisfying while for the quadrupole moment they are not satisfying at all. There seems to be an important error either in our model or in our measured quadrupole moment and it could be induced by different factors. However, since both curves coincide well for the monopole moment, there shouldn't be an important error in one of our cosmological parameter. As explained previously, because both curves present a similar behaviour for $s > 25\text{Mpc}/h$, the problem is quite intriguing and couldn't be found in this project. Regardless of that, we can make the assumption that the discrepancy comes from an integration imprecision or from the size of our bins for the separation vector s . It would be interesting to compute the model using different size of bins. It would have been also more precise to include on the data of Fig. 7 the uncertainty values as errorbars which we could have obtain using the covariant matrix of our measurements.

Furthermore, we wanted to verify (3) in order to make sure our computation of $\Delta(r)$ is correct as well as to be confident when using

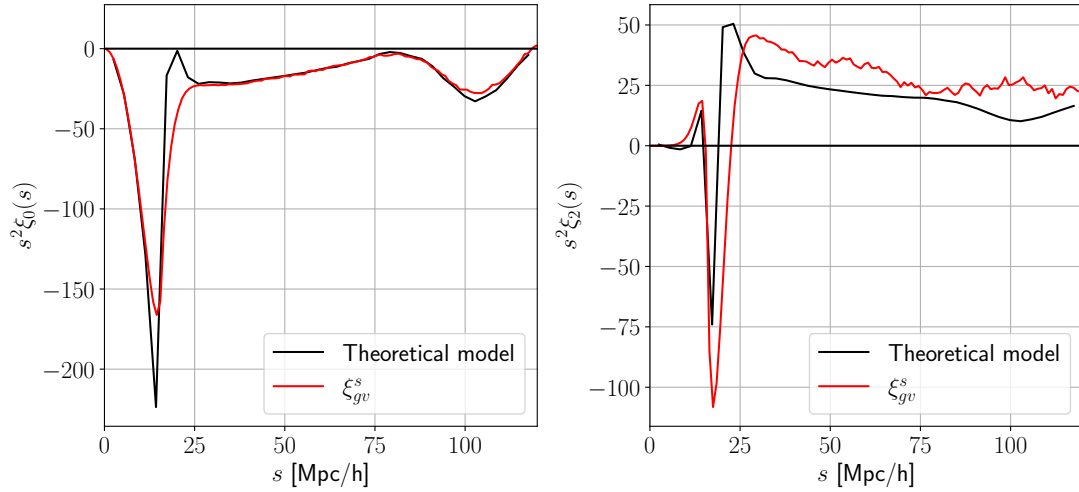


Figure 7. Measured multipoles of the redshift space void-galaxy cross-correlation ξ_{vg}^s multiplied by s^2 as a function of the radial void-galaxy separation s . Left : The monopole $\xi_0^s(s)$. Right: The quadrupole $\xi_2^s(s)$. In both panels, the solid curve shows the theoretical prediction for our full linear model including velocity dispersion.

$v_r = -\frac{1}{3}faH\Delta(r)r$ in (9). In order to do that, we tried to compute the galaxy velocity projected on the separation vector r given by :

$$v_g(r) = \frac{1}{N_{vg}} \sum_{i,j} \mathbf{v}_j \cdot \hat{\mathbf{r}}_{ij} \quad (10)$$

where $\hat{\mathbf{r}}_{ij}$ is the real space separation vector between the i th void and j th galaxy and \mathbf{v}_j the velocity of that galaxy, and the sum runs over all N_{vg} void-galaxy pairs with $\|\mathbf{r}_{ij}\|$ in the range $(rdr, r + dr)$. The computation of v_g seemed to be close to $-\frac{1}{3}faH\Delta(r)r$ but as we weren't sure we decided to not include any comparison of both functions. We thus considered (3) to hold and used it when computing our theoretical model (8). However, in case there is a discrepancy because of an error in $\Delta(r)$, this could lead to an error in the construction of the model. This could explain the problem we encounter with the quadrupole moment in Fig. 7.

Finally, it would also be interesting for our project to slightly change our Λ CDM model by taking a different value for the Hubble constant. Here the simulation used took $H = 67.77\text{km/s/Mpc}$ but recent cosmology studies have found different values for the measured value of H and the disagreement is now highly statistically significant such that the discrepancy is referred as the Hubble tension. For example, the Planck Mission in 2018 found $H = 67.74 \pm 0.46\text{km/s/Mpc}$, The LIGO Scientific Collaboration and The Virgo Collaboration in 2017 found $H = 70.0^{+12.0}_{-8.0}\text{km/s/Mpc}$ while recent Hubble Space Telescope measurements in 2020 found $H = 72.1 \pm 2.0\text{km/s/Mpc}$. The results obtained with a Big MultiDark simulation with different cosmological parameters could be different from the ones we found and interesting to study.

6 CONCLUSION

Throughout this project, we have provided a measurement of the anisotropic void-galaxy cross-correlation $\xi_s(s)$ using void and galaxy catalogues at redshift $z = 0.5$ in the Big MultiDark simulation. This measurement is found to be an useful tool for cosmologists to test for possible environmental dependence of the growth rate of

structures. We also computed an RSD model for the void-galaxy correlation in redshift space using linear dispersion theory which was developed and improved in previous scientific papers.

By comparing our model prediction to the measurements, we have seen how the model provides an excellent fit to the data of our N-body simulation results on all scales for the monopole moment while the computation of the quadrupole moment needed some improvements.

REFERENCES

- B. Delaunay *Izvestia Akademii Nauk SSSR O. M. i. E. N.*,
 Betancort-Rijo J., Patiri S. G., Prada F., Romano A. E., 2009, *MNRAS*, **400**, 1835
 Cai Y.-C., Taylor A., Peacock J. A., Padilla N., 2016, *MNRAS*, **462**, 2465
 Matsubara T., 2008, *Phys. Rev. D*, **78**, 109901
 Nadathur S., Percival W. J., 2019, *MNRAS*, **483**, 3472
 Nadathur S., Hotchkiss S., Crittenden R., 2017, *MNRAS*, **467**, 4067
 Nadathur S., Carter P. M., Percival W. J., Winther H. A., Bautista J. E., 2019a, *Phys. Rev. D*, **100**, 023504
 Nadathur S., Carter P., Percival W. J., 2019b, *MNRAS*, **482**, 2459
 Peacock J. A., et al., 2001, *Nature*, **410**, 169
 Scoccimarro R., 2004, *Physical Review D*, **70**
 Sutter P. M., Pisani A., Wandelt B. D., Weinberg D. H., 2014, *MNRAS*, **443**, 2983
 Zhao C., Tao C., Liang Y., Kitaura F.-S., Chuang C.-H., 2016, *MNRAS*, **459**, 2670